Electrodeposition of Bi-Te Alloy Films

Makoto Takahashi, Youichi Oda, Takayuki Ogino, and Shinsaku Furuta

Department of Industrial Chemistry, Chubu University, Matsumoto-cho 1200, Kasugai, Aichi 487, Japan

ABSTRACT

Electrochemical deposition of Bi-Te alloy films from acidic solutions containing $Bi(NO_3)_3$ and TeO_2 has been investigated. The thickness, compound, and composition of the Bi-Te alloy films have been examined using stylus-type surface profiling techniques, x-ray diffraction peak measurement, and inductively coupled plasma/Auger electron spectroscopy measurements. At potentials where limiting current was observed, the compositions of films were controlled by the mole ratio $[Bi^{3+}]/[HTeO_2^+]$ in the solutions and the relationship between the composition of electrodeposited films and the composition of electrolyte solutions was derived.

Bismuth telluride (Bi_2Te_3) and the Bi-Te solid solution alloy have been of considerable interest as thermoelectric materials,[1] a key element of an optical storage system,[2] *et cetera*.

Growing tendency towards miniaturization in many fields has augmented an interest in thin film products and technologies. Thermoelectric devices, *e.g.*, modules for cooling laser diodes,[3] were also miniaturized to remain compatible with smaller devices.

Bismuth telluride thin films have been prepared mainly by vacuum evaporation.[4,5] The electrochemical deposition may offer a low cost growth method of high quality metal and semiconductor thin films. But the preparation of bismuth telluride thin films and bismuth tellurium alloy thin films by electrochemical deposition have not been reported.

We have investigated the electrodeposition of CdTe thin films and reported the effect of the deposition conditions (*e.g.*, deposition potential and the composition of solution) on the composition and the electronic and photoelectrochemical properties of the films.[6-8]

In this paper, we report the electrodeposition of bismuth telluride thin films and the correlation between the deposition conditions and the composition of the films.

Experimental

Bismuth-tellurium alloy films were cathodically deposited from aqueous solutions of pH 1.0-0.7 containing $Bi(NO_3)_3$ and TeO_2 on Ti sheets (The Nilaco Company, Limited, 0.3 mm thick). These substrates were degreased by chloroform and ethanol solutions and then washed by deionized water before use. A potentiostat (Hokuto Denko, HA-301) was used to control the electrode potential. The reagent grade HNO_3, Bi_2O_3 (purity 99.9%), and TeO_2 (purity 99%) were used without further purification. Water was purified by Milli Q water purification system. The usual three-electrode cell was used for the deposition of Bi-Te alloy films. A platinum wire and an Ag/AgCl electrode (3.33 mol/liter KC1) were used as a counterelectrode and a reference electrode, respectively. The current-potential relations were obtained potentiostatically by using a potentiostat and a X-t recorder (TOA Electronic Limited, Model FBR-252A). The electrochemical measurements and the deposition of the films were carried out at room temperature after the electrolyte solutions were deaerated by passing Ar gas through the solution for about 15 min.

X-ray diffraction, the thickness of films, and inductively coupled plasma/Auger electron spectroscopy (ICP/AES) measurements were carried out by using a Rigaku Denki RAD-1B x-ray diffractometer, Kosaka Laboratory Limited Surfcorder Model SE-3F, and Jarrell Ash Plasma Atom Comp 90-975, respectively.

Results

The current-potential relation of a Ti sheet electrode in a solution containing 1.50 m*M* TeO_2 and 1.50 m*M* $Bi(NO_3)_3$ is shown in Fig. 1. The cathodic current increased at potentials more negative than 0.05 V *vs.* Ag/AgC1 and black products were deposited on the Ti sheet electrode surface. The limiting current was observed at potentials between −0.20 and −0.35 V. This limiting current was affected by the concentration of $Bi(NO_3)_3$ and TeO_2. The cathodic current increased rapidly at potentials more negative than −0.40 V and many bubbles were formed on the electrode surface.

The current-potential relation of a Ti sheet electrode in a solution containing 7.50 m*M* $Bi(NO_3)_3$ is shown in Fig. 2. The cathodic current increased at potentials more negative than 0.05 V and gray products were formed on the electrode surface. The limiting current was observed at potentials between −0.15 and −0.30 V. The cathodic current increased rapidly at potentials more negative than −0.35 V, and many bubbles were formed on the electrode surface. The observed limiting current was affected by $Bi(NO_3)_3$ concentration and the dependence of the limiting current density on the $Bi(NO_3)_3$ concentration is shown in Fig. 2. The limiting current increased linearly with the increase of $Bi(NO_3)_3$ concentration. This limiting current was affected by the stirring rate. Thus the observed limiting current is a diffusion current for a process limited by Bi^{3+} ion diffusion.

The current-potential relation in a solution containing 1.03 m*M* TeO_2 is shown in Fig. 3. The cathodic current increased at potentials more negative than 0 V and gray products were formed on the electrode surface. The limiting current was observed at potentials between −0.20 and −0.35 V. This limiting current was proportional to the TeO_2 concentration and the stirring rate as expected for a process limited by $HTeO_2^+$ ion diffusion.

The dependences of limiting current on the $Bi(NO_3)_3$ concentration for the solutions in which TeO_2 concentrations

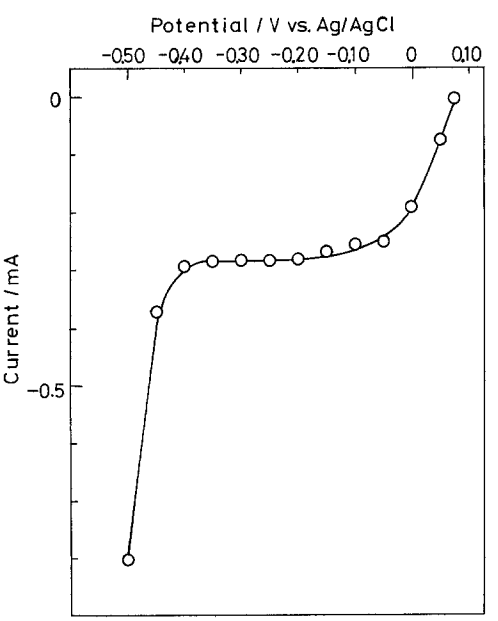

Fig. 1. Current-potential relation of Ti electrode in a nitric acid solution (pH 0.90) containing 1.50 m*M* $Bi(NO_3)_3$ and 1.50 m*M* TeO_2. Electrode area: 0.94 cm^{-2}.

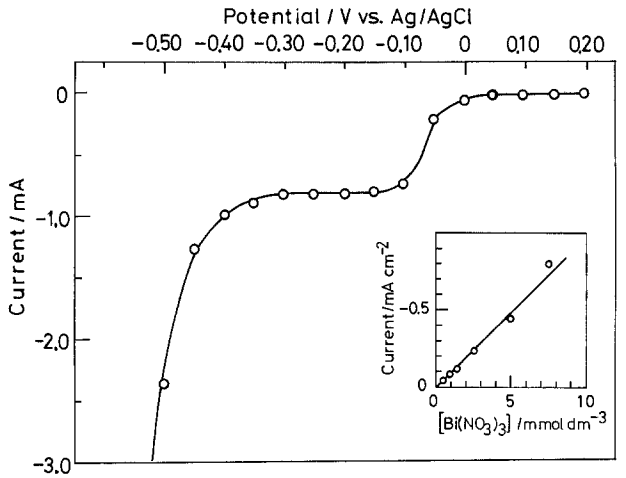

Fig. 2. Current-potential relation of Ti electrode in a nitric acid solution (pH 0.82) containing 7.50 m*M* $Bi(NO_3)_3$. Electrode area: 0.94 cm^{-2}. Insert: dependence of the limiting current on the $Bi(NO_3)_3$ concentration at −0.25 V (*vs.* Ag/AgCl).

were kept constant (a) 1.50, (b) 0.50, and (c) 0.00 m*M* are shown in Fig. 4. For each case, the limiting current is proportional to the $Bi(NO_3)_3$ concentration. The slope of these plots have the same value (0.083 ± 0.006). Therefore the limiting current for the diffusion of $Bi(NO_3)_3$ is not affected by the existence of Te atoms on the electrode surface and $HTeO_2^+$ in the solution. The values of the intercepts for the plot were the same values observed in Fig. 3. The limiting current observed in the solution containing TeO_2 and $Bi(NO_3)_3$ is the sum of limiting currents observed for TeO_2 and $Bi(NO_3)_3$, respectively. Therefore Bi and Te atoms are independently deposited on the electrode surface.

The plot of the average film thickness against the charge passed during the deposition, Q_{dep} is shown in Fig. 5. The film thickness linearly increased with the increase of Q_{dep}. The uniformity of the thickness throughout the films was ±15%.

X-ray diffraction patterns of the films deposited from the solutions containing 1.50 m*M* TeO_2 and various $Bi(NO_3)_3$ concentrations (a) 0.15, (b) 1.20, and (c) 1.50 m*M* are shown in Fig. 6. In the x-ray diffraction pattern, (Fig. 6a), the diffraction peaks at 2θ = 23.02°, 27.58°, 38.17°, 40.48°,

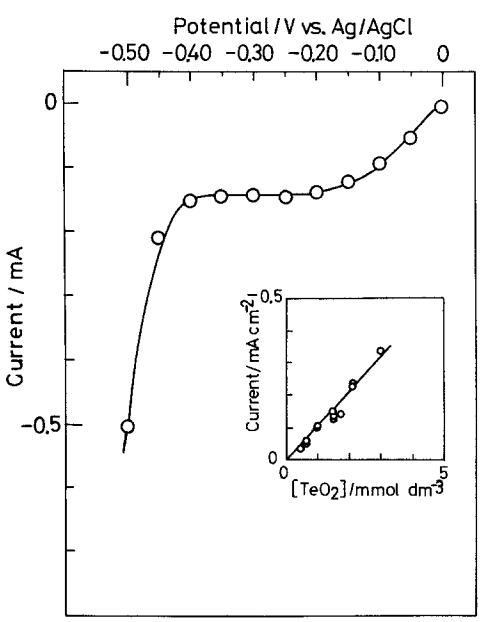

Fig. 3. Current-potential relation of Ti electrode in a nitric acid solution (pH 0.92) containing 1.03 m*M* TeO_2. Electrode area: 0.94 cm^{-2}. Insert: dependence of the limiting current on the TeO_2 concentration at −0.25 V (*vs.* Ag/AgCl).

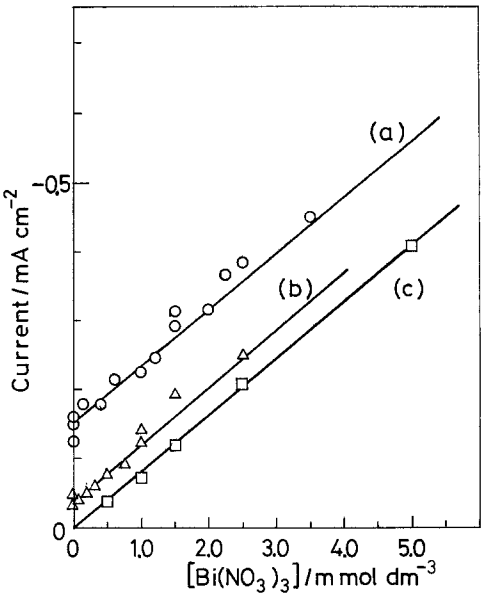

Fig. 4. The dependence of the limiting current at −0.25 V (*vs.* Ag/AgCl) on $Bi(NO_3)_3$ concentration for the nitric acid solution (pH 0.90 ± 0.10) containing various concentrations of TeO_2: (a) 1.50, (b) 0.50, and (c) 0.00 m*M*.

43.25°, 49.58°, and 56.92° corresponded to (100), (101), (102), (110), (111), (201), and (202) plane of Te metal.[9] In the x-ray diffraction pattern (b), the broad diffraction peaks were observed at 2θ = 23.60°, 27.65°, 38.04°, 41.13°, and 49.82°, and these peaks had shoulders. These observed peaks corresponded to peaks for Bi_2Te_3 [10] or $Bi_{2+x}Te_{3-x}$, [11] and the positions of the shoulders corresponded to the diffraction peaks for Te metal. It is suggested that the film consisted of the mixture of Te metal and Bi-Te alloy compounds (*e.g.*, Bi_2Te_3, $Bi_{2+x}Te_{3-x}$). The diffraction peaks for the film deposited from the solution containing 1.50 m*M* $Bi(NO_3)_3$ and 1.50 m*M* TeO_2 were observed at 2θ = 17.50°, 23.60°, 27.68°, 37.83°, 40.09°, 45.30°, 50.35°, and 57.28°. These diffraction peaks corresponded to the diffraction peaks of Bi_2Te_3 or $Bi_{2+x}Te_{3-x}$.

The mole ratio Bi/Te of the films deposited from the solution containing 1.50 m*M* TeO_2 and various concentrations of $Bi(NO_3)_3$ were determined by ICP/AES measurements. The plots of the mole ratio Bi/Te of the films against the $Bi(NO_3)_3$ concentration in the electrolyte solution are shown in Fig. 7. The mole ratio Bi/Te of the films linearly

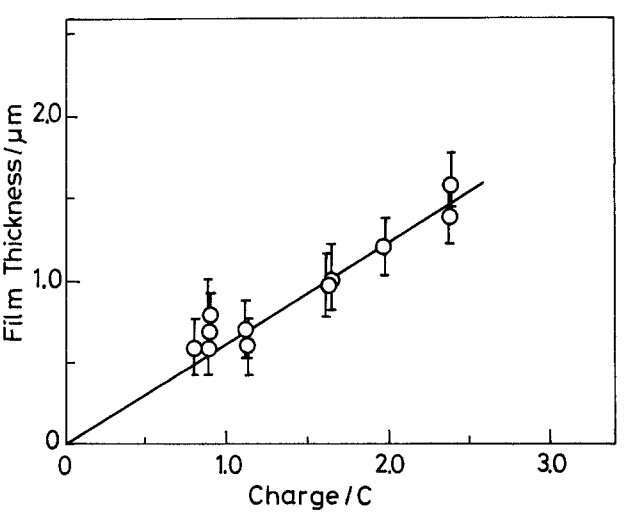

Fig. 5. The average thickness of the electrochemically deposited films on Ti as a function of charge passed. The deposition was carried out at −0.25 V (*vs.* Ag/AgCl) in a nitric acid solution (pH 0.90 ± 0.20) containing 1.50 m*M* TeO_2 and 0.60 m*M* $Bi(NO_3)_3$.

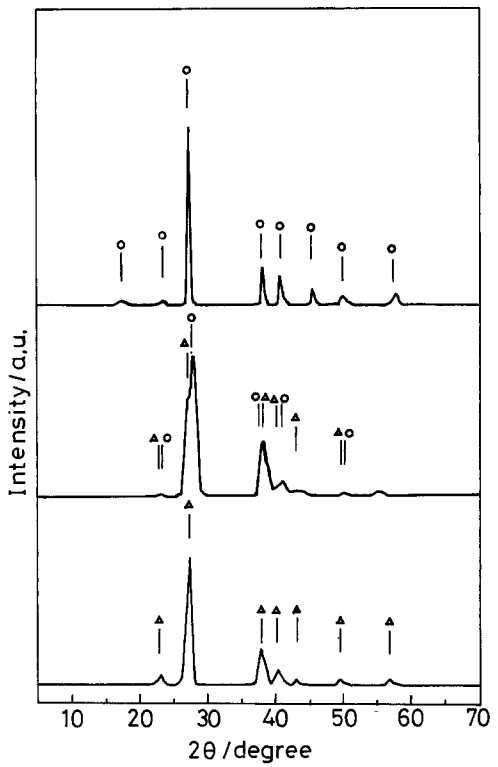

Fig. 6. X-ray diffraction patterns of the films deposited from the nitric acid solution (pH 0.90 ± 0.20) containing 1.50 m*M* TeO_2 and various concentrations of $Bi(NO_3)_3$: (a) 0.15, (b) 1.20, and (c) 1.50 m*M*. Deposition potential was −0.25 V *vs.* Ag/AgCl. (○) Bi_2Te_3 (or $Bi_{2+x}Te_{3-x}$), (△) Te metal.

increased with the increase of $Bi(NO_3)_3$ concentration. Therefore it is suggested that the composition of the films can be controlled by the mole ratio $[Bi(NO_3)_3]/[TeO_2]$ in the solution, when the films are deposited in the limiting current potentials.

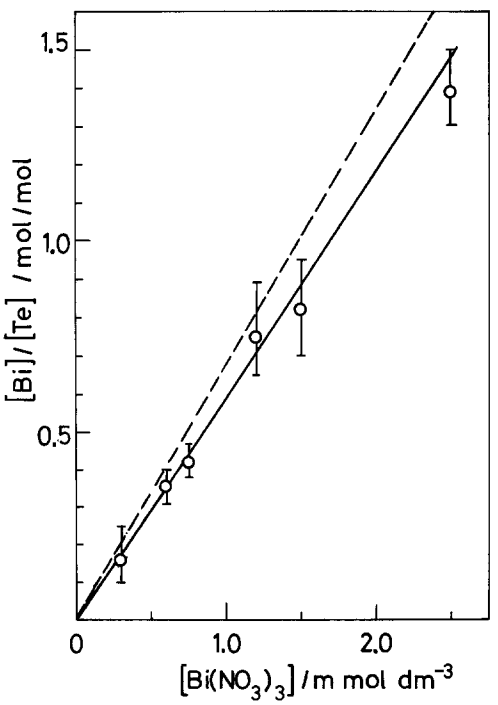

Fig. 7. The mole ratio Bi/Te of the electrochemically deposited films (solid line) as a function of $Bi(NO_3)_3$ concentration in the electrolytic solution. TeO_2 concentration was 1.50 m*M*. Deposition potential was −0.25 V *vs.* Ag/AgCl. Dotted line corresponds to the relationship predicted by Eq. 10.

Discussion

In the limiting current potentials, the following reactions were involved in the formation of Bi-Te alloy compounds.

Electrode reaction

$$Bi^{3+} + 3e^- \rightarrow Bi(s)^{12} \quad [1]$$

$$HTeO_2^+ + 3H^+ + 4e^- \rightarrow Te(s) + 2H_2O^{13} \quad [2]$$

Solid state reaction

$$mBi(s) + nTe(s) \rightarrow Bi_mTe_n(s) \quad [3]$$

The limiting currents due to reaction 1 and 2 are given by Eq. 4 and 5 respectively

$$i_{Bi} = -\frac{3D_{Bi}FC_{Bi^{3+}}}{\delta_{Bi^{3+}}} \quad [4]$$

$$i_{Te} = -\frac{4D_{Te}FC_{HTeO_2^+}}{\delta_{HTeO_2^+}} \quad [5]$$

where D_{Bi} (D_{Te}), $\delta_{Bi^{3+}}$, ($\delta_{HTeO_2^+}$), and $C_{Bi^{3+}}$ ($C_{HTeO_2^+}$) are the diffusion coefficient, the thickness of diffusion layer, and the bulk concentration of Bi^{3+} ($HTeO_2^+$), respectively. Therefore the observed limiting current for the solution containing Bi^{3+} and $HTeO_2^+$ is expressed by Eq. 6

$$i_{obs.} = i_{Bi} + i_{Te} = -\frac{3D_{Bi}FC_{Bi^{3+}}}{\delta_{Bi^{3+}}} - \frac{4D_{Te}FC_{HTeO_2^+}}{\delta_{HTeO_2^+}} \quad [6]$$

This is supported by the results presented in Fig. 4. At deposition time, t(s), the number of moles of Bi and Te in the film are expressed by

$$n_{Bi}(mol) = i_{Bi}t/(3F) = \frac{D_{Bi}C_{Bi^{3+}}t}{\delta_{Bi^{3+}}} \quad [7]$$

and

$$n_{Te}(mol) = i_{Te}t/(4F) = \frac{D_{Te}C_{HTeO_2^+}t}{\delta_{HTeO_2^+}} \quad [8]$$

respectively. Accordingly the relationship between the mole ratio Bi/Te in the film and the mole ratio $[Bi^{3+}]/[HTeO_2^+]$ in the solution is given by Eq. 9

$$\frac{n_{Bi}}{n_{Te}} = \frac{D_{Bi}\delta_{HTeO_2^+}C_{Bi^{3+}}}{D_{Te}\delta_{Bi^{3+}}C_{HTeO_2^+}} \quad [9]$$

The values of $D_{Bi}/\delta_{Bi^{3+}}$ and $D_{Te}/\delta_{HTeO_2^+}$ are given by the slopes of the plots in Fig. 2 and 3, respectively. Using the obtained values, Eq. 9 can be rewritten as Eq. 10

$$\frac{n_{Bi}}{n_{Te}} = \frac{1.03C_{Bi^{3+}}}{C_{HTeO_2^+}} \quad [10]$$

The dotted line in Fig. 7 corresponds to the mole ratio Bi/Te of the film calculated using Eq. 10. The calculated values agree reasonably with the experimental data. Brenner *et al.*[14] classified the electrodeposition of alloys into five groups. The case in which the composition of the deposited film is controlled by the diffusion of the ions was named "regular codeposition." Therefore the electrodeposition of Bi-Te alloy films in this study is classified as regular codeposition.

The products observed in this study and the products expected from the phase diagram[15] for the same Te concentration [mole percent, (m/o)] are summarized in Table I. The products in the films were different from those expected from the phase diagram. According to the phase diagram, the eutectic phase (Te metal and Bi_2Te_3) exists for compositions above 60.4 m/o Te. But for the deposited film the eutectic phase was observed for compositions extending from 57.5 to 71.0 m/o Te. At 54.9 m/o Te, though the peritectic phase (BiTe) was observed in the phase diagram, Bi_2Te_3

Table I. The composition and products of electrodeposited films and products expected from the phase diagram.

Te concentration (m/o)	Electrodeposited products	Products expected from the phase diagram
90.9	Te	Te + Bi_2Te_3
87.0	Te	Te + Bi_2Te_3
71.0	Te + Bi_2Te_3 (or $Bi_{2+x}Te_{3-x}$)	Te + Bi_2Te_3
57.5	Te + Bi_2Te_3 (or $Bi_{2x}Te_{3-x}$)	BiTe
54.9	Bi_2Te_3 (or $Bi_{2+x}Te_{3-x}$)	BiTe

or $Bi_{2+x}Te_{3-x}$ was observed, and the peritectic phase was not observed in the deposited films. These results can be explained as follows. The electrodeposition process for this study consists of the following three steps: (*i*) the diffusion of ions from the bulk solution to the electrode surface and the adsorption of ions on the electrode surface, (*ii*) the reduction of adsorbed ions at the electrode surface, (*iii*) the migration of reduced atoms to the reactive points and the solid-state reaction.

Since the electrodeposition was done in the potential region in which the current was limited by diffusion, step (*ii*) seems to proceed rapidly and step (*i*) is rate-determining. Steps (*i*) and (*ii*) affect the composition of the film. But step (*iii*) does not affect the composition and mainly affect the products and crystallinity of the film. It is known that the velocity of the migration and the solid-state reactions increase with increase of the temperature.[16] In this study, since the electrodeposition was done at room temperature, the migration velocity of reduced atoms seems to be slow, so that the solid-state reaction 3 expected from the phase diagram cannot proceed completely and the electrodeposited products are different from the products expected from the phase diagram. In fact, the peritectic phase (BiTe) was observed in the film deposited from the solution containing 1.50 m*M* TeO_2 and 1.50 m*M* $Bi(NO_3)_3$ at 75°C.

Acknowledgments

Dr. T. Hattori of Toyohashi University of Technology, Aichi, is acknowledged for his help in ICP/AES measurements.

Manuscript submitted Feb. 9, 1993; revised manuscript received May 26, 1993.

Chubu University assisted in meeting the publication costs of this article.

REFERENCES

1. (a) H. J. Goldsmid and R. H. Douglas, *Br. J. Appl. Phys.*, **5,** 386 (1954); (b) T. Ohta, T. Uesugi, T. Tokiai, M. Nosaka, and T. Kajikawa, *Trans. IEE Jpn.*, **111-B,** 670 (1991).
2. D. Y. Lou, *Appl. Opt.*, **21,** 1602 (1982).
3. (a) S. Hava, H. B. Sequeira, and R. G. Hunsperger, *J. Appl. Phys.*, **58,** 1727 (1985); (b) T. Okoshi and K. Kikuti, *Electron Lett.*, **16,** 179 (1980).
4. K. Borkowski and J. Przyluski, *Mater Res. Bull.*, **22,** 381 (1987).
5. F. Vollklein, V. Baier, U. Dillner, and E. Kessler, *Thin Solid Films,* **187,** 253 (1990).
6. M. Takahashi, K. Uosaki, and H. Kita, *This Journal,* **131,** 2304 (1984).
7. M. Takahashi, K. Uosaki, and H. Kita, *ibid.,* **133,** 266 (1986).
8. M. Takahashi, K. Uosaki, and H. Kita, *J. Appl. Phys.*, **60,** 2046 (1986).
9. ASTM X-ray Power Data, 4-554.
10. ASTM X-ray Power Data, 15-863.
11. ASTM X-ray Power Data, 8-27.
12. M. Pourbaix, *Atlas d'Equilibres Electrochimiques,* p. 536, Gauthiers Villars et Cie, Paris (1963).
13. M. P. R. Panicker, M. Knaster, and F. A. Kroger, *This Journal,* **125,** 566 (1978).
14. A. Brenner, *Electrodeposition of Alloys 1,* p. 76, Academic Press, New York (1963).
15. A. C. Glatz, *This Journal,* **112,** 1204 (1965).
16. K. Mochizuki, YI Xinjian, and T. L. Chu, *J. Crystal Growth,* **67,** 420 (1984).